

Power quality improvement of grid-connected photovoltaic systems using PI-fuzzy controller

Marwan Saded Ahmed, Dhari Yousif Mahmood, Ali Hussein Numan

Department of Electrical Engineering, University of Technology, Baghdad, Iraq

Article Info

Article history:

Received Sep 4, 2021

Revised Mar 5, 2022

Accepted Mar 24, 2022

Keywords:

Five levels H-bridge inverter

Photovoltaic grid-connected

PI-fuzzy controller

Power quality

THD

ABSTRACT

To ensure enhanced reliability and availability of electricity to consumers, grid-connected photovoltaic systems need to improve their power quality, this paper uses a three-phase five levels cascaded H-bridge inverter in grid-connected mode to improve the flexibility and efficiency of the photovoltaic system. Each photovoltaic (PV) array in the proposed system has a maximum power point tracker (MPPT) to extract the PV array maximum power point for a particular irradiance and temperature and reduce the mismatch that causes an imbalance in the power sent from the inverter to the main grid. The fuzzy logic controller is used to tune the proportional-integral (PI) controller to regulate the current and voltage of the grid-connected inverter by changing the gain of the PI controller (K_p , K_i) to obtain a fast response and improve the power quality of the system despite different load disturbances and inputs. The system was simulated in MATLAB/Simulink, and the results show the superiority of the proposed control unit, in which a pure and stable sine output voltage and current waveforms. Finally, the total harmonic distortion (THD) is improved to reach 3.81% based on the fuzzy PI controller, while 7.77% is based on the PI controller.

This is an open access article under the [CC BY-SA](https://creativecommons.org/licenses/by-sa/4.0/) license.



Corresponding Author:

Marwan Saded Ahmed

Department of Electrical Engineering, University of Technology, Baghdad, Iraq

Email: marwanesd448@gmail.com

1. INTRODUCTION

Many countries nowadays rely heavily on wind energy and solar panel energy as a source of renewable energy (RES), especially with the spread and development of technology, being more reliable and sustainable to form a microgrid integrated with the traditional grid and solve the problem of increasing energy demand and reducing dependence on fossil fuel and environmental conservation [1].

Energy management and the conversion of renewable energy generated (RES) into electricity and its storage, requires the use of electronic devices as power converter systems and must be ideal in configuration and size and meet the requirements for optimum operation of microgrid in terms of high efficiency, performance, reliability, stability, low cost, protection, and effective energy regulation [2], [3]. One of the most important electronic power converters, which is an inverter. An inverter can be defined as an electronic device that converts DC power into AC power while maintaining the output voltage and frequency. Inverters are divided into two types: the first type is a two-level inverter, and the second is a multilevel inverter with three levels or more [3].

Because of the high switching losses, high switching frequency, harmonic distortion, and other problems in the two-level inverter as it cannot be used in high and medium voltage transformations, the engineers of electronic power and modern technology have tended to pay attention to and use the multilevel inverter because of its many advantages and high capacity to deal with medium and high energy with its

positive contribution in the field of renewable energy and electronic capacity. Multilevel inverters are classified into three classes [3], [4]: i) flying capacitor multilevel inverter, ii) cascaded H-bridge multilevel inverter, and iii) diode clamped multilevel inverter.

This paper presents an inverter topology of five levels H-bridge cascaded connected to the utility grid with reliance on photovoltaic panels as a DC source. one of the most important problems facing this system is the mismatch of the photovoltaic panel, as each photovoltaic (PV) module gives its power (maximum power point (MPP)) due to the change of irradiance and temperature or consumption of the photoelectric board. So, the powers supplied to the inverter are unbalanced, resulting imbalance in the injection of grid current to achieve equilibrium; the modulation must be compensated, so a control scheme is presented for each PV module in the system. Therefore, any module can be dispensed with when shading or any defect occurs in the module on the other hand, the traditional control technique deals with linear systems and is affected by disturbances [5]. Therefore, fuzzy logic control (FLC) techniques that are non-linear have been proposed approach because it includes three main sources from nonlinearity, i.e. base rule, inference engine and jamming units this fuzzy logic-based control model is proven to be a successful approach to the control of many non-linear it has been suggested as an alternative approach for conventional control techniques (PI) and compare the results between the two methods [6]. Many studies have relied on the method of the fuzzy logic controller for use with the photovoltaic system as [6]–[9]. The fuzzy logic control algorithm (PI-fuzzy) is used to control the current and voltage of the grid-connected inverter by changing the gain (Ki, Kp) of the PI controller, improving the efficiency of the PV system [7]–[10].

2. DESCRIPTION OF THE SYSTEM

The cascaded H-bridge multilevel inverter connected to a three-phase grid, using solar panels as a DC voltage source, the system connected to the utility grid via an L filter to filter unwanted signals as well as transformers for isolation and protection. Figure 1 shows the components of the system.

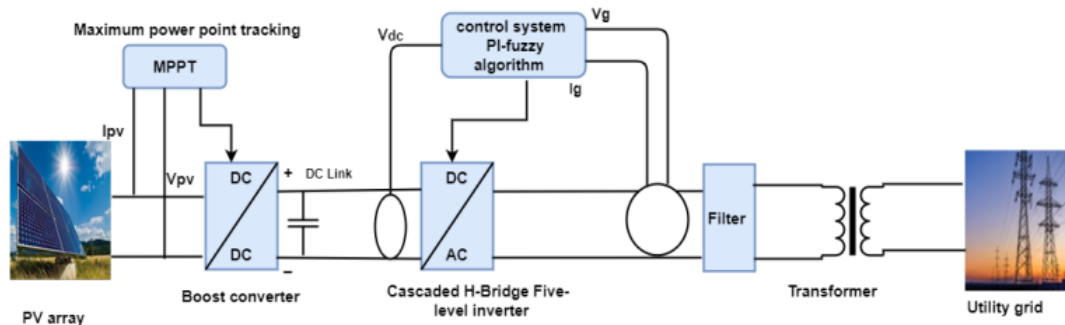


Figure 1. Components of a proposed PV system

2.1. PV array

The solar cell is the basic unit for forming PV panels. A solar cell can be defined as a semiconductor material that converts solar radiation into electrical energy, the solar cell consists of a thin layer of a semiconductor material that is fabricated on a PN junction such as silicon, cadmium telluride, gallium arsenide, etc, its operational properties are similar to that of a diode p-n as it relies on solar radiation and surface temperature to generate electrical current. A photovoltaic cell can generate almost voltage 0.5 to 0.8 volt depending on the advanced technology and type of semiconductor material used [11].

The voltage generated by a single solar cell is insufficient for the applications, so the solar cells are connected in one frame in series and parallel to their component called the solar panel. The equivalent circuit of a solar cell can consist of a single or double diode, and a single diode is more efficient and easier to analyse. Figure 2 shows the equivalent circuit of a solar cell with a single diode [10], [11]. The relationship between output voltage (V_{PV}) and output current (I_{PV}) in the equivalent circuit of a single diode can be analysed mathematically as (1) [12].

$$I_{PV} = I_{ph} - I_D - I_{sh} \quad (1)$$

Where:

I_{PV} : Current of PV cell (A)

I_{ph} : Photo-current (A); generated by the photoelectric effect

I_D : Diode current (A)

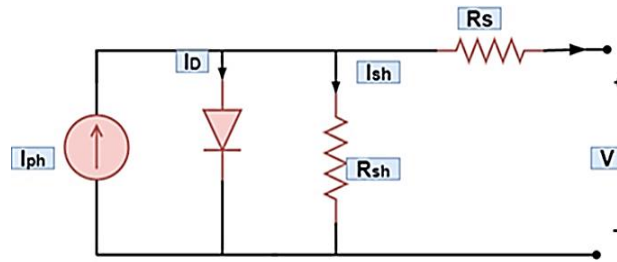


Figure 2. Equivalent circuit of a single diode solar cell

The (2) shows the dependence of the voltage and current of the solar cell on radiation level, temperature, and their changes.

$$I_{ph} = I_{SC} + K_i(T - T_r)(G/G_{nom}) \quad (2)$$

Where:

I_{SC} : short circuit current (A)

K_i : short circuit current of a cell at (STC) standard test condition 25 °C and 1000 W/m².

T : operating temperature (K)

T_r : Reference temperature of the PV cell (298.15 K)

G : Solar radiation in W/m²

G_{nom} : Nominal solar radiation 1000 W/m²

$$I_0 = I_{rs} \left[\frac{T}{T_r} \right]^3 \exp(q \times E_{go}) / (AK) \left(\frac{1}{T} \right) - \left(\frac{1}{T} \right) \quad (3)$$

$$I_{rs} = I_{scr} / \exp(qV_{oc}) / (N_s KAT) - 1 \quad (4)$$

Where:

I_0 : Reverse saturation current

I_{rs} : Cell reverse saturation current at T_r .

q : The charge of the electron is equal to 1.6×10^{-19} coulomb

E_{go} : bandgap energy of the semiconductor = 1.1 e V

A : The ideality factor of the diode

K : Boltzmann's constant equal 1.3805×10^{-23} J/k

V_{oc} : Open circuit voltage

N_s : number of cells connected in series

Now, the output current of the PV cell is in the (5) and (6).

$$I_{PV} = I_{ph} - I_0 \left[\exp(q \times V_{PV} + I_{PV} \times R_s) / (N_s AKT) - 1 \right] + I_{sh} \quad (5)$$

and

$$I_{sh} = (V + I_{PV} R_s) / R_{sh} \quad (6)$$

Where:

R_s : series resistance (Ω)

R_{sh} : shunt resistance (Ω)

V_{PV} : Output voltage from PV panel

The energy that is practically used to power the loads [8]. The (7) represents the relationship between I-V in the PV array.

$$I_{PV} = N_p \times I_{ph} - N_p \times I_0 \left\{ \exp \left[\frac{(V_{PV} + \frac{N_s}{N_p} I_{PV} R_s)}{N_s AKT} \right] \right\} - 1 + \frac{V \frac{N_s}{N_p} + I_{PV} R_s}{R_{sh}} \quad (7)$$

Where:

N_p : number of PV modules connected in parallel

N_s : number of PV modules connected in series

2.2. Boost converter

The boost converter is called a step-up converter because the output voltage is greater than the input voltage, Figure 3 shows the structure of the boost converter which consists of two semiconductors (diode and MOSFET), and the inductor which is the power storage source in addition to the capacitance such as the filter, load impedance and DC voltage source (PV array or battery).

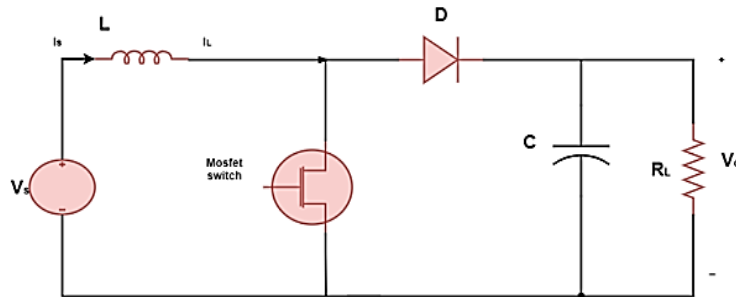


Figure 3. Circuit diagrams of the boost converter

The MOSFET is used as a trigger switch in the circuit, and the boost switch operates in two modes. The first is when the switch is closed in the ON position, the current is stored in the inductor for a certain period and the diode prevents the current from flowing. With the load current remaining constant due to capacitor discharge. In the second position, when the switch is opened, current flows through the inductor and diode, and the capacitor is charged and from there to the load while the load current also remains constant [13]. Using Faraday's law, the relationship between the output and input voltage of the boost converter can be found as shown in (8) [14].

$$V_s \cdot DT = (V_o - V_s)(1 - D)T \quad (8)$$

Where:

V_s : input voltage

V_o : output voltage of DC-DC boost converter

D : Duty cycle

2.3. Incremental conductance algorithm (INC)

Figure 4 represents a flowchart of the INC algorithm, features of this algorithm include the speed of processing steady-state errors, rapid response to variable solar radiation, as well as the speed of convergence, as it combines accuracy and speed. The maximum power point in the PV matrix is traced from the derivation of the relationship $P \cdot V$ concerning voltage or current. MPP can be calculated using the dp/dv and $-I/v$ relationship and as shown by the following derivation:

$$P = V \times I \quad (9)$$

$$\frac{dP}{dv} = I + V \cdot \frac{dI}{dv} \quad (10)$$

or

$$\frac{dP}{dI} = V + I \cdot \frac{dv}{dI} \quad (11)$$

From the calculation to depend on the values I and V , the MPP values can be inferred from the following expressions:

$\frac{\Delta I}{\Delta V} > \frac{-I}{V}$ The operating point is to the left of MPP

$\frac{\Delta I}{\Delta V} = \frac{-I}{V}$ The operating point is exactly at MPP

$\frac{\Delta I}{\Delta V} < \frac{-I}{V}$ The operating point is to the right of MPP

According to these comparisons, the algorithm increases or decreases the voltage in the PV array [15], [16].

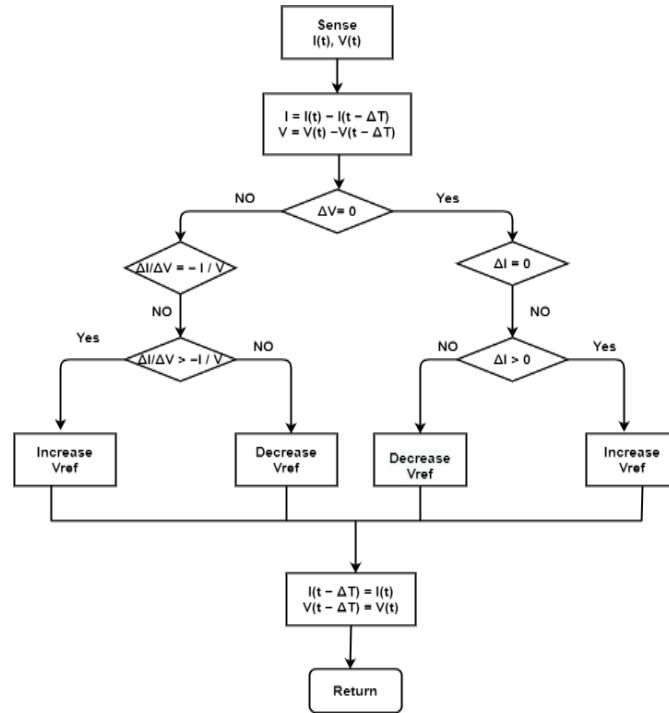


Figure 4. Flowchart of INC algorithm

2.4. Cascaded H-bridge inverter

Cascaded H-bridge are several single-phase inverters or called H-bridge inverters connected in series, each bridge consists of an independent DC source in addition to switches, as shown in Figure 5. This inverter generates a sinusoidal output voltage as each H-bridge provides three levels (zero, positive output voltage, negative output voltage). The total output voltage is the sum of all the voltages produced by the connected H-bridge cells in the chain. Where if the number of H-bridge cells is M the total output voltage is equal to (2M+1). High power quality reduced harmonic distortion, low switching losses, high-quality output wave are among the main advantages of this inverter [4], [10].

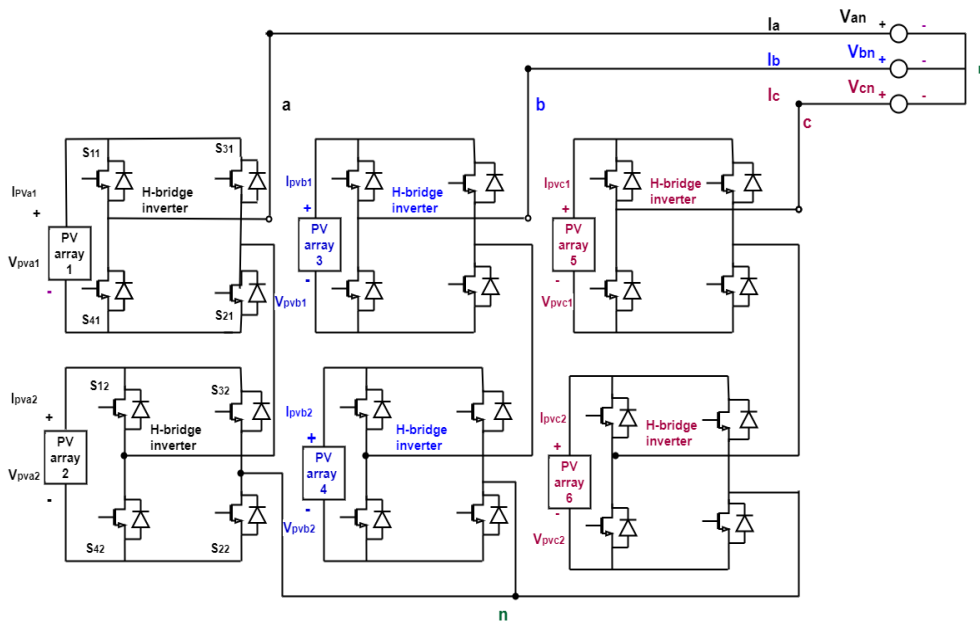


Figure 5. Topology of the modular cascaded H-bridge multilevel inverter for a three-phase grid-connected PV system

3. CONTROL SCHEME

One of the most important problems facing the PV system is the mismatch of the PV panels due to the uneven radiation and temperature changes in addition to the lifetime of the solar panels, which means that the MPP is different for each PV model. This reduces the efficiency of the photovoltaic system and the occurrence of problems in the three-phase system at each stage due to the lack of current balance in the grid, so there must be a maximum power point tracker (MPPT) for each PV array independently, control and synchronization between the grid and the system [5], [17], [18].

The control process consists of two closed loops, an inner control loop that regulates the current and an external control loop that controls the DC voltage regulation, maintains a constant DC link voltage, and produces signals to the inner control loop as a reference for the current. Changes in conditions affecting the PV array (radiation and temperature) result in a difference in the power produced from it which reaches the utility grid via the DC link. Therefore, the power produced does not match the power that reaches the utility grid, hence the voltage control unit provides a match between the power produced from the PV array and the power delivered to the utility grid by changing the active power of the reference current [19], [20].

The inner control unit (current) can be designed with different frames of reference which are synchronous (dq), fixed frames (αβ), and natural frames (abc). It should be capable of harmonic compensation, grid synchronization, active and reactive power control with a fast-dynamic response. Since the inverter used is three-phase multilevel, a combination of variable AC signals is used, namely, grid current (Iabc) and grid voltage (Vabc), as well as converting these variable quantities from natural frame (abc) to synchronous frame (dq). Therefore, Clark or Park transformations are required to be used for this purpose, depending on the phase-locked loop (PLL) to estimate the synchronization angle.

The control unit (dq) independently controls the active and reactive power by component current (d) for active power and component current (q) for reactive power, to get the unit power factor, component (q) is controlled and made equal to zero and thus the control process becomes easier after the disengagement between the two components (P and Q) and relying on PI-fuzzy controller for its advantages to make the system more efficient, Where the proposed PI-fuzzy controller is used in the external control loop to stabilize the incoming voltage of the inverter and optimize the wave coming out from the inverter so that it is sine and pure, and is also used in the inner loop of current to improve power quality and reduce THD [7], [19], [21]. The scheme shown in Figure 6 represents the MPPT single control and control circuit for the proposed system.

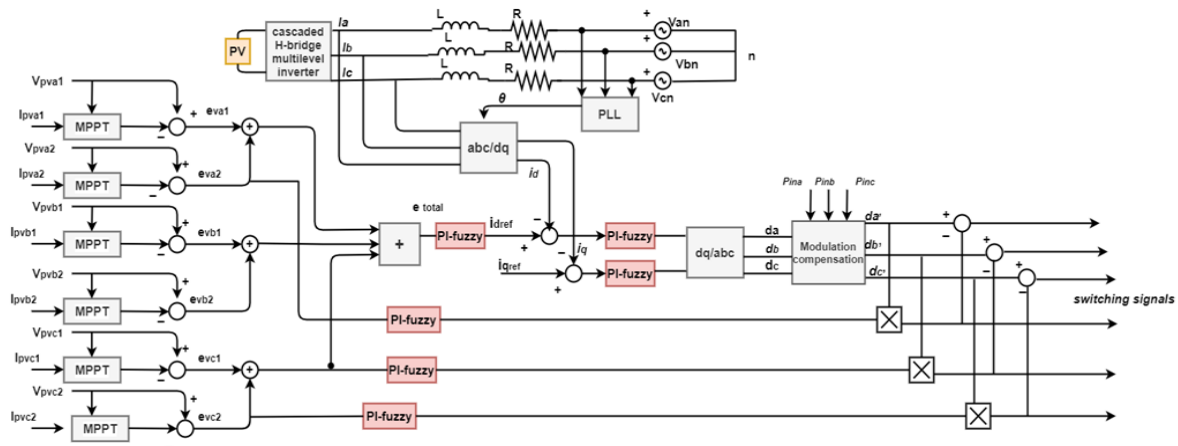


Figure 6. Control scheme for three-phase five-level cascaded H-bridge multilevel inverter

Park transformation (13) and (14) are applied to convert voltage and current from nature frames into a synchronous reference frame (dq) [22].

$$\begin{bmatrix} V_d \\ V_q \end{bmatrix} = \frac{\sqrt{2}}{\sqrt{3}} \begin{bmatrix} \sin(\omega t) & \sin\left(\omega t - \frac{2\pi}{3}\right) & \sin\left(\omega t + \frac{2\pi}{3}\right) \\ \cos(\omega t) & \cos\left(\omega t - \frac{2\pi}{3}\right) & \cos\left(\omega t + \frac{2\pi}{3}\right) \end{bmatrix} \begin{bmatrix} V_a \\ V_b \\ V_c \end{bmatrix} \quad (13)$$

$$\begin{bmatrix} I_d \\ I_q \end{bmatrix} = \frac{\sqrt{2}}{\sqrt{3}} \begin{bmatrix} \sin(\omega t) & \sin\left(\omega t - \frac{2\pi}{3}\right) & \sin\left(\omega t + \frac{2\pi}{3}\right) \\ \cos(\omega t) & \cos\left(\omega t - \frac{2\pi}{3}\right) & \cos\left(\omega t + \frac{2\pi}{3}\right) \end{bmatrix} \begin{bmatrix} I_a \\ I_b \\ I_c \end{bmatrix} \quad (14)$$

4. FUZZY LOGIC CONTROLLER

The non-linear behavior of most real systems and the difficulty in modelling them is one of the most important problems facing these systems, as classical controllers (PID, PI, P) which are feedback controllers deal with fixed parameters, so they are not adapt with the environment variables and changes in the parameter system, as well as the setting of parameters for the controller is difficult since an accurate mathematical model is usually hard to obtain to adjust these parameters and solve these problems, So it is necessary suitable control unit that adapts to various change. Fuzzy logic control is an intelligent control method that uses fuzzy rule sets and linguistic representations of a human's knowledge to control a plant. It is an important branch of intelligent control. Positive control effects have been obtained using fuzzy logic technology in a variety of control fields. The essence of FLC is converting expert knowledge of related fields and the experience of skilled operators into language rules, and then using fuzzy reasoning and fuzzy decision-making to implement complex system control. The proposed controller (fuzzy-PI) is applied to the outer control loop of the dc link to reduce the ripples of the dc-link, as well as to the two inner double current loops (Id and Iq); i) The design process for an FLC entails determining the inputs, ii) establishing the rules, and iii) devising a method for demulsifying the fuzzy result of the rules into an output signal, known as defuzzification. Figure 7 shows the Structure of the fuzzy PI controller [8], [9].

4.1. Design fuzzy-PI

4.1.1. Determine the input and output

The deviation e and the change of error are the FLC's inputs. The FLC constantly checks and calculates the inputs, and then the PI controller's parameters are adjusted online using fuzzy logic rules to achieve optimal parameters. Error e and error change rate can satisfy the requirements of PI parameter self-tuning at different times as FLC inputs in the fuzzy adaptive PI controller. Each of the input signals has seven membership functions, while each of the output signals has seven. From Figure 7 a block diagram of the proposed FLC algorithm with the input and output changes, wherein the input signals are the error current in the d-q frame and the derivation of the regulated voltage is as follows:

$$e_{Id} = G_i (id_{ref} - id) \tag{15}$$

$$e_{Iq} = G_i (iq_{ref} - iq) \tag{16}$$

$$e_{Vd} = G_v (Vd_{ref} - Vd) \tag{17}$$

Where:

G_v and G_i : gain factors to unify the input signal per-unit (pu)

V_d, V_q & I_d, I_q : Voltage and current variables in rotating reference frame

V_{d_ref} & V_{q_ref} : Voltages reference at d-axis and q-axis

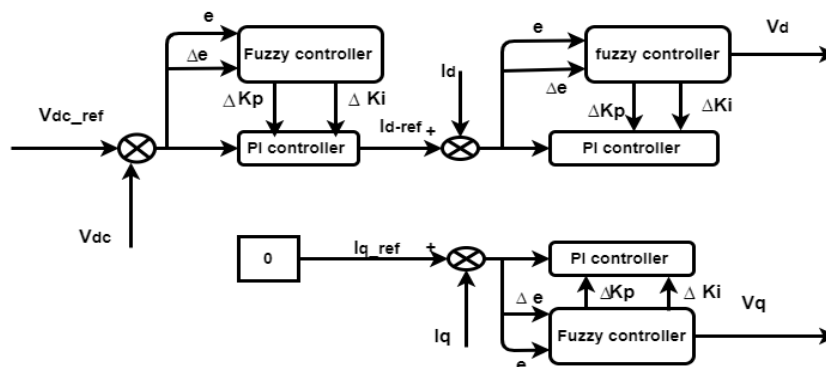


Figure 7. Structure of the PI-fuzzy controller

Figure 8(a) and 8(b) (see Appendix) depicts the design of the input membership functions of variables and the proportional gain K_p and the integral gain K_i membership functions are designed as shown in Figure 9(a) and 9(b) (see Appendix). Simple normalization calculations yield the fuzzy set domain ranges

of input and output variables. The input variables' fuzzy set domain is set to e, $\Delta e = \{-1, 0, 1\}$ and the fuzzy set domain of outputs $\Delta K_p, \Delta K_i$ are set as (-1, 1) and (-1, 1) respectively. The input and output variables for the corresponding fuzzy sets are set as follows: e, $\Delta e, \Delta K_p, \Delta K_i = \{NB, NM, NS, ZE, PS, PM, PB\}$. The fuzzy sets' means are referred to as negative big (NB), negative medium (NM), negative small (NS), zero (ZE), positive small (PS), positive medium (PM), and positive big (PB).

4.1.2. Fuzzification and fuzzy reasoning

The normal distribution applies to all fuzzy variables. The Mamdani type is used in the fuzzy inference system, as follows: If e is A and Δe is B, then u is c. Tables 1 and 2 show the fuzzy logic rules for the output variables, respectively.

Table 1. Rule-base fuzzy of ΔK_i parameter

ΔK_i	Δe							
	NB	NM	NS	ZE	PS	PM	PB	
e	NB	NB	NM	NM	NS	ZE	ZE	
	NM	NB	NB	NM	NS	NS	ZE	
	NS	NB	PM	NS	NS	ZE	PS	
	ZE	NM	NM	NS	ZE	PS	PM	
	PS	NM	NM	ZE	PS	PS	PM	
	PM	ZE	ZE	PS	PS	PM	PB	
	PB	ZE	ZE	PS	PM	PB	PB	

Table 2. Rule-base fuzzy of ΔK_p parameter

ΔK_p	Δe							
	NB	NM	NS	ZE	PS	PM	PB	
e	NB	PB	PB	PM	PM	PS	ZE	
	NM	PB	PB	PM	PS	PS	ZE	
	NS	PM	PM	PM	PS	ZE	NS	
	ZE	PM	PM	PS	ZE	NS	NM	
	PS	PS	PS	ZE	NS	NS	NM	
	PM	PS	ZE	NS	NM	NM	NB	
	PB	ZE	ZE	NM	NM	NM	NB	

4.1.3. Defuzzification

Defuzzification entails devising a method for converting the rules' fuzzy results into output signals. To obtain accurate FLC output, the weighted average method is used. The following is a description of the weighted average method:

$$u_0 = \frac{\sum_{i=1}^n u_i \mu_c(u_i)}{\sum_{i=1}^n \mu_c(u_i)} \tag{19}$$

Online self-tuning of PI controller parameters the proposed self-tuning of PI parameters aims to uncover the hazy relationship between two PI parameters and FLC inputs. The DC-link voltage V_{dc} is sensed and compared to the reference DC-link voltage V_{dcref} to implement the FLC algorithm of the grid-connected in a closed loop. The FLC continuously checks and calculates the deviations e and Δe to meet the control parameters of different requirements for different e and Δe . The PI controller's parameters are then adjusted online using fuzzy rules to achieve an excellent dynamic and static performance for the PV system. The self-tuning of parameters is based on the processing of fuzzification results, fuzzy reasoning, and defuzzification. The PI controller's parameter regulation formula is used to achieve the goal of online regulation.

$$Kp_{-punew} = Kp + \Delta K_p \tag{20}$$

$$Ki_{-punew} = Ki + \Delta K_i \tag{21}$$

5. SIMULATION RESULTS AND DISCUSSION

The cascade multilevel grid-connected inverter simulation was done using the MATLAB/Simulink platform. Via an inductor filter and interface transformer, the inverter is coupled to the grid. Table 3 presents the parameters of the PV array. For both irradiation and temperature fluctuations MPP set-point monitoring, detailed simulation investigations were conducted to objectively analyze the performances. For profiles where differences in MPP set-point monitoring are such that the full range of irradiation and temperature values are used, a good controller is needed. In this section, the simulation results are carried under shading conditions with (500 W/m², 1000 W/m²) irradiation and (25 °C, 32 °C) temperature. The PV system is comprising of six groups and each group has 54 panels, two panels in series, and 28 panels in parallel, and the output voltage of one PV array is 109.4 volts, as well as the output current of the PV group, is 156.24 A. The photovoltaic power output is approximately 17 Kw. The input DC voltage for a single-phase of inverter which is including two H-bridge is 500 V.

There are two periodic in the profile used for this test case. For the first periodic (t=0-1.2 s), the irradiation is reduced to 500 W/m² and the temperature is maintained at STC (25 °C). while in the second periodic (t=1.2-2s), the irradiation level returns to the maximum irradiation 1000 W/m² and the temperature is increased to 32 °C, as shown in Figures 10-16.

Table 3. Electrical parameters of the PV panel

Parameters	Values
Maximum power (Pmax)	305 w
Rated Voltage (Vmp)	54.7 V
Rated Current (Imp)	5.58 A
Open Circuit Voltage (Voc)	64.2 V
Short Circuit Current (Isc)	5.96 A
Number of cells in the panel	96

The output voltage of five levels injected into the main grid by the proposed converter during controlled operation based on the fuzzy PI and PI controller are shown in Figures 10(a) and 10(b). The proposed controller based on fuzzy with CHB has a five-level output voltage waveform that is very stable and has no overshoot as compared with the PI controller which is depicted in Figure 10(b). While the output voltage of the proposed system after the L filter based on the fuzzy PI and PI controller is shown in Figures 11(a) and 11(b). It is obvious from the results in this figure, the output voltage is having high stability and it has a pure sine wave without a ripple at the steady-state region. In Figure 12, the output of AC currents of fuzzy PI and PI controller is showing. It is obvious from the waveforms in this figure, the waveform of three-phase AC currents based on the fuzzy PI is a pure sine wave and no overshoot with a high steady-state as compared with the PI controller which has high ripples and lower stability at the steady-state region as shown in Figure 12(b).

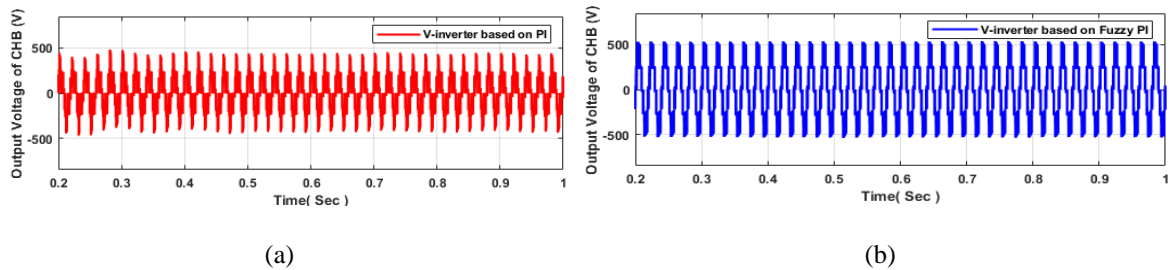


Figure 10. Waveforms of output voltage of the inverter, (a) output voltage of five-level CHB based on PI controller, (b) output voltage of five-level CHB based on fuzzy PI

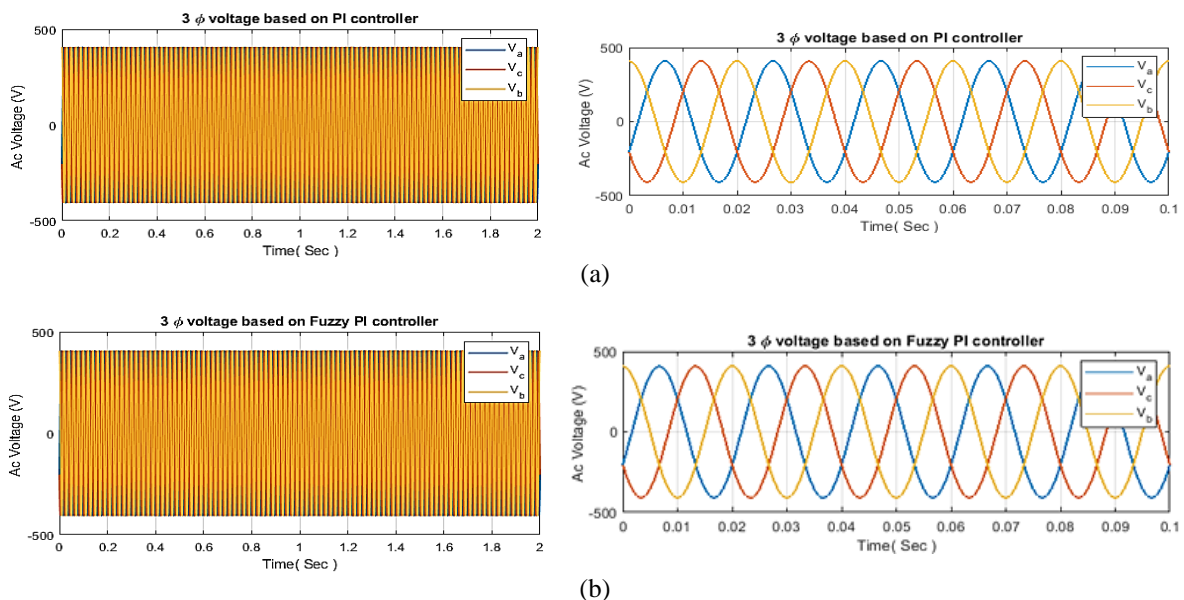


Figure 11. Waveforms of AC load side after L filter: (a) output voltage of AC bus based on PI controller with zoom and (b) output voltage of AC bus based on the fuzzy PI controller with zoom

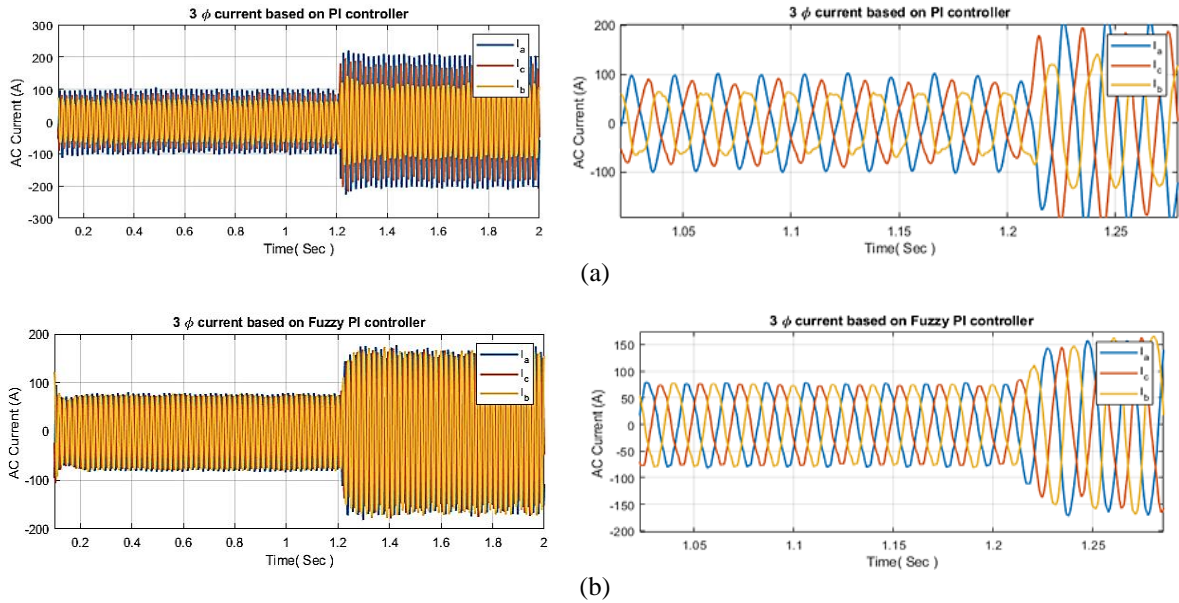


Figure 12. Waveforms of AC load side after L filter: (a) output current of AC bus based on PI controller with zoom and (b) output current of AC bus based on the fuzzy PI controller with zoom

While the output power of PV groups and output power of AC side load based on the fuzzy PI controller is very tracking to the maximum power desired and no oscillation at the steady-state region as compared with PI controller at (500 W/m², 25 °C), as well as in (1000 W/m², 32 °C) as shown in Figures 13(a) and 13(b). The DC link voltage waveform has been depicted in Figure 14. It is obvious from this figure; the voltage remains constant which implies the system is very stable and rejected the disturbances.

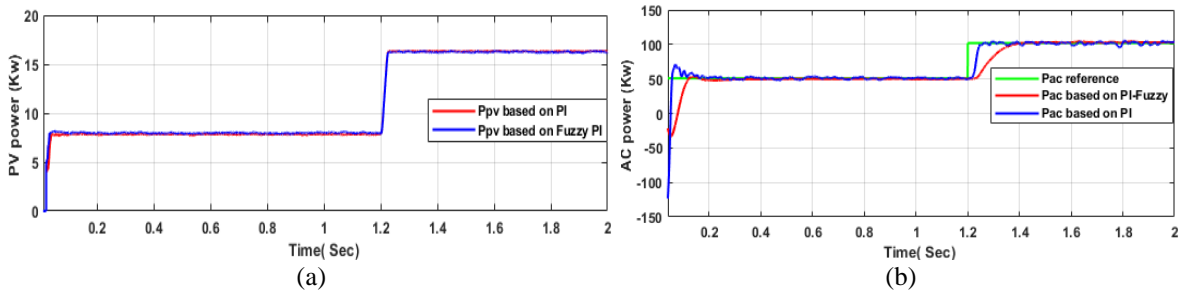


Figure 13. Responses of output power: (a) output power of PV array for one group and (b) output power of AC side

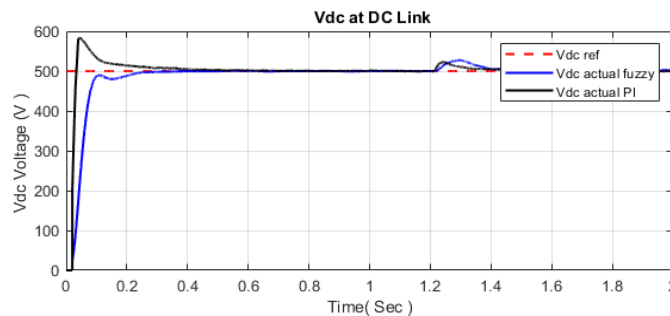


Figure 14. Response of DC voltage after boost converter

The values of the PI controller of the five-level inverter based on the fuzzy system for DC voltage controller and current controller have been depicted in Figures 15(a) and 15(b). Finally, to show the superiority of the proposed control based on a fuzzy system in improved the power quality of the proposed system, the harmonics analysis based on fast Fourier analysis for THD is depicted in Figures 16(a) and 16(b). It can be seen in this figure, the percentage THD for AC current is 3.81% while the THD is equal to 7.77% which proved the superiority of the proposed PI controller in enhancement the power quality of the overall system and increased the reliability of the system.

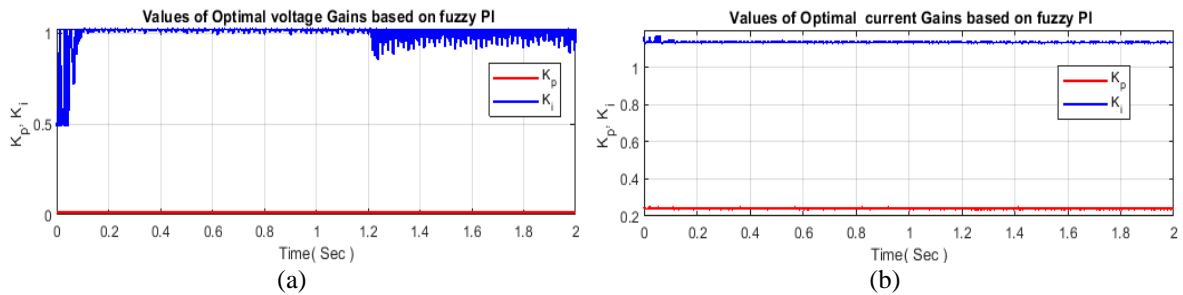


Figure 15. Values of PI parameters based on fuzzy system: (a) values of PI parameters of DC voltage controller and (b) values of PI parameters of the current controller

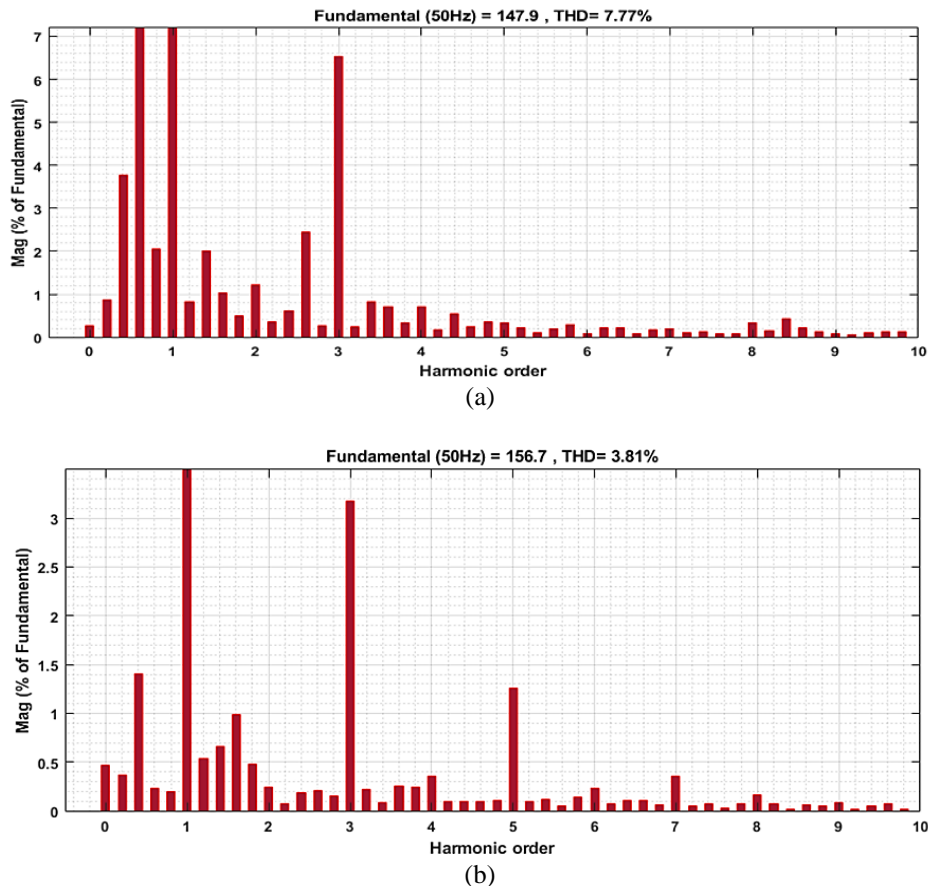


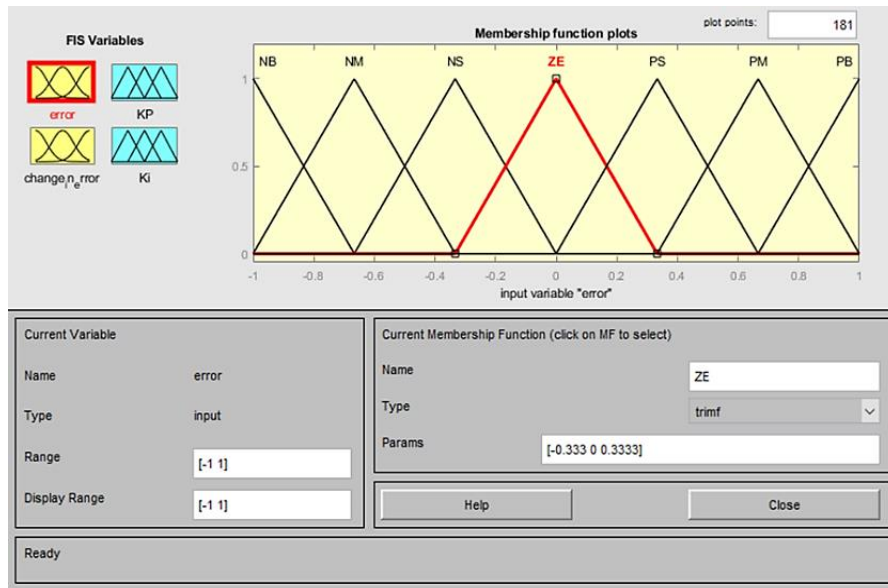
Figure 16. THD percentage for AC current: (a) THD percentage using PI controller and (b) THD percentage using a PI-fuzzy controller

6. CONCLUSION

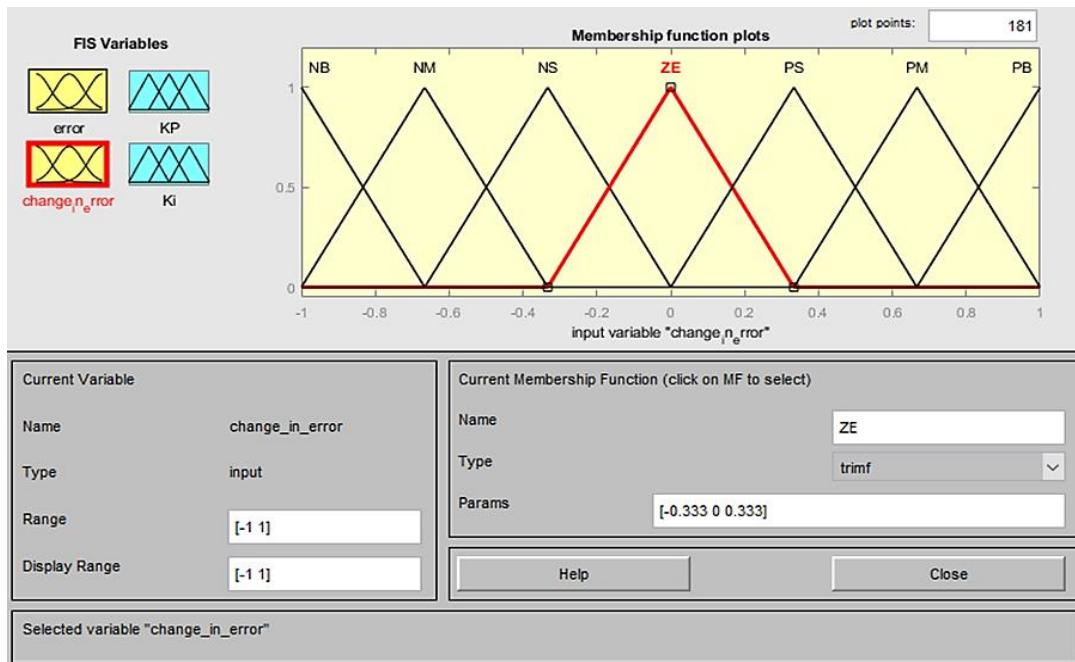
This paper describes a modified connection using a five-level cascade H-bridge inverter with six PV groups system that avoids mismatch by separating each PV group with a DC-DC converter and MPPT to

reach the maximum output power of six PV groups to achieve the design power of 100 Kw and PI-fuzzy controller has been proposed to control the DC voltage controller and the Idq current controller. The results showed that the output voltage waveform is stable and has a pure sine wave without a ripple in the steady-state region, as well as the waveform for three-phase AC currents based on the fuzzy PI is a pure sine wave and there is no overshoot with the high steady-state as compared to the PI controller. Finally, the total harmonic distortion (THD) is reduced in the AC currents from 7.77% to 3.81 % in the proposed system, which means the fuzzy PI controller has increased the reliability and stability of the system and its rejection of disturbances, and achieved the desired expectations in improving power quality.

APPENDIX

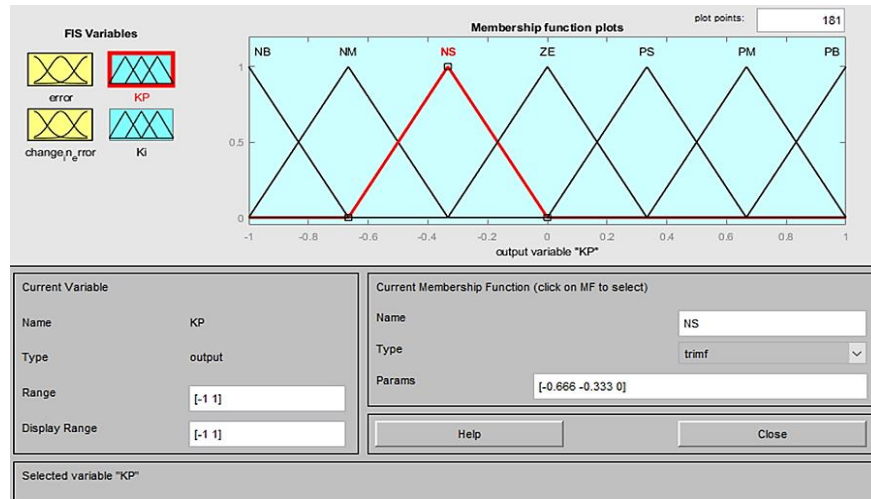


(a)

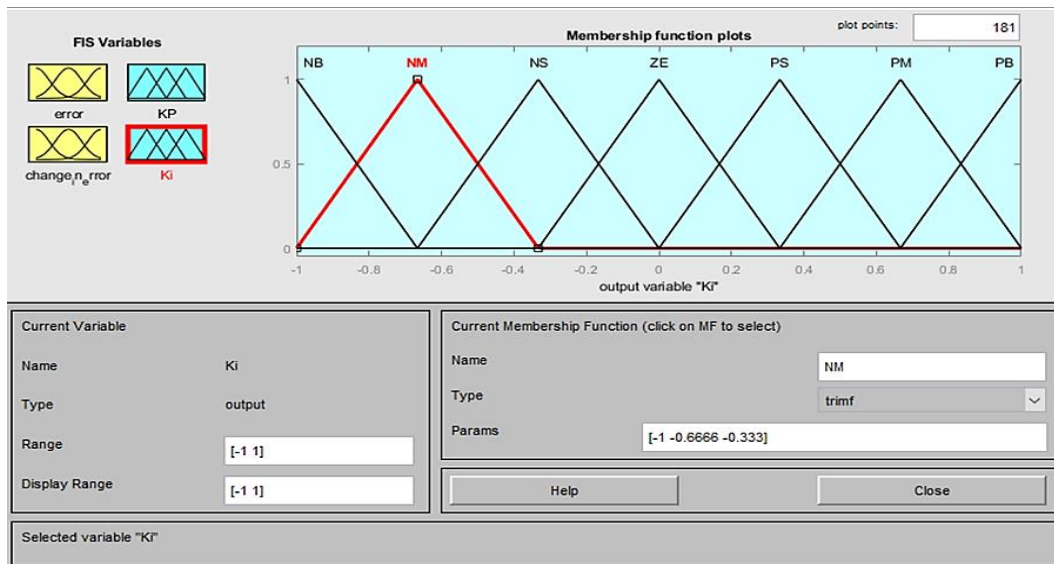


(b)

Figure 8. Fuzzy subgroups of the input signals: (a) error and (b) change of error



(a)



(b)

Figure 9. Fuzzy subgroups of the output signals: (a) linguistic output changes (Kp) and (b) linguistic output changes (Ki)

REFERENCES

- [1] P. Ray and M. Biswal, Eds., *Microgrid: Operation, control, monitoring and protection*, Lecture No. Springer, 2020. [Online]. Available: <https://link.springer.com/book/10.1007/978-981-15-1781-5>
- [2] S. Bayhan, H. Abu-Rub, J. I. Leon, S. Vazquez, and L. G. Franquelo, "Power electronic converters and control techniques in AC microgrids," in *IECON 2017 - 43rd Annual Conference of the IEEE Industrial Electronics Society*, Oct. 2017, pp. 6179–6186. doi: 10.1109/IECON.2017.8217073.
- [3] L. Castro, S. Perez-Londono, and J. Mora-Florez, "Application of Fuzzy Logic based Control in Micro-grids," in *2019 FISE-IEEE/CIGRE Conference - Living the energy Transition (FISE/CIGRE)*, Dec. 2019, pp. 1–8. doi: 10.1109/FISECIGRE48012.2019.8985002.
- [4] A. Krishna R and L. P. Suresh, "A brief review on multi level inverter topologies," in *2016 International Conference on Circuit, Power and Computing Technologies (ICCPCT)*, Mar. 2016, pp. 1–6. doi: 10.1109/ICCPCT.2016.7530373.
- [5] I. H. Shanono, N. R. H. Abdullah, and A. Muhammad, "A survey of multilevel voltage source inverter topologies, controls, and applications," *Int. J. Power Electron. Drive Syst.*, vol. 9, no. 3, p. 1186, Sep. 2018, doi: 10.11591/ijpeds.v9.i3.pp1186-1201.
- [6] D. Tamilarasi and T. S. Sivakumaran, "Fuzzy PI control of symmetrical and asymmetrical multilevel current source inverter," *Int. J. Fuzzy Syst.*, vol. 20, no. 2, pp. 426–443, Feb. 2018, doi: 10.1007/s40815-017-0352-8.
- [7] N.-T. Nguyen and H.-H. Lee, "Fuzzy PI Controller for Grid-Connected Inverters," in *Lecture Notes in Computer Science*, Springer, 2012, pp. 300–308. doi: 10.1007/978-3-642-25944-9_39.
- [8] O. Z. Bakhoda, M. B. Menhaj, and G. B. Gharehpetian, "Fuzzy logic controller vs. PI controller for MPPT of three-phase grid-connected PV system considering different irradiation conditions," *J. Intell. Fuzzy Syst.*, vol. 30, no. 3, pp. 1353–1366, Mar. 2016, doi: 10.3233/IFS-152049.
- [9] A. Kaysal and R. Bayindir, "Design and Analysis of Fuzzy Logic Controllers for Microgrid Voltage Control," in *2018 2nd International Symposium on Multidisciplinary Studies and Innovative Technologies (ISMSIT)*, Oct. 2018, pp. 1–6. doi:

- 10.1109/ISMSIT.2018.8567258.
- [10] S. S. Katkamwar and V. R. Doifode, "Cascaded H-bridge multilevel PV inverter with MPPT for grid connected application," in *2016 International Conference on Energy Efficient Technologies for Sustainability (ICEETS)*, Apr. 2016, pp. 641–646. doi: 10.1109/ICEETS.2016.7583832.
- [11] T. S. Kishore, S. D. Kaushik, and Y. Venu Madhavi, "Modelling, Simulation and Analysis of PI and FL Controlled Microgrid System," in *2019 IEEE International Conference on Electrical, Computer and Communication Technologies (ICECCT)*, Feb. 2019, pp. 1–8. doi: 10.1109/ICECCT.2019.8869379.
- [12] X. H. Nguyen and M. P. Nguyen, "Mathematical modeling of photovoltaic cell/module/arrays with tags in Matlab/Simulink," *Environ. Syst. Res.*, vol. 4, no. 1, p. 24, Dec. 2015, doi: 10.1186/s40068-015-0047-9.
- [13] N. Ramalingam *et al.*, "Implementation of PI controller for boost converter in PV system," *Int. J. Adv. Res. Manag. Archit. Technol. Eng.*, vol. II, no. April, pp. 6–10, 2016.
- [14] M. H. Rashid, *Power Electronics Handbook*. Butterworth-Heinemann, Elsevier, 2017.
- [15] F. L. Tofoli, D. de Castro Pereira, and W. J. de Paula, "Comparative study of maximum power point tracking techniques for photovoltaic systems," *Int. J. Photoenergy*, vol. 2015, pp. 1–10, 2015, doi: 10.1155/2015/812582.
- [16] R. I. Putri, S. Wibowo, and M. Rifa'i, "Maximum power point tracking for photovoltaic using incremental conductance method," *Energy Procedia*, vol. 68, pp. 22–30, Apr. 2015, doi: 10.1016/j.egypro.2015.03.228.
- [17] A. Lashab *et al.*, "Cascaded multilevel PV inverter with improved harmonic performance during power imbalance between power cells," *IEEE Trans. Ind. Appl.*, vol. 56, no. 3, pp. 2788–2798, May 2020, doi: 10.1109/TIA.2020.2978164.
- [18] M. M. Paul Raj and S. S. Meenakshi Sundaram, "Cascaded H-bridge five-level inverter for grid-connected photovoltaic system Using proportional-integral controller," *Meas. Control (United Kingdom)*, vol. 49, no. 1, pp. 33–41, 2016, doi: 10.1177/0020294016629175.
- [19] N. M. Mohsin, "Design of a Grid Connected Photovoltaic Power Electronic Converter," 2017. [Online]. Available: <http://www.bioone.org/doi/abs/10.3159/10-RA-011.1>
- [20] D. Y. Mahmood, A. H. Numan, and J. K. Ateih, "Simple and efficient control method for battery charging in high penetration photovoltaic array," no. May, pp. 1813–1819, 2019.
- [21] Rajan J. Devi and Supriya S. Kadam, "Synchronization of three phase inverter with electrical grid," *Int. J. Eng. Res.*, vol. V4, no. 05, May 2015, doi: 10.17577/IJERTV4IS050938.
- [22] G. J. May, A. Davidson, and B. Monahov, "Lead batteries for utility energy storage: A review," *J. Energy Storage*, vol. 15, pp. 145–157, Feb. 2018, doi: 10.1016/j.est.2017.11.008.

BIOGRAPHIES OF AUTHORS



Marwan Saded Ahmed     is an M.Sc. degree student in the research level at Electrical Engineering Department, University of Technology, Baghdad, Iraq, and complete a B.Sc. degree in 2009 in the Electrical Engineering Department, University of Dyala, Dyala, Iraq. Mr. Marwan is interested in Power Electronic Converters, PV Systems, Microgrid systems, and Storage Energy Systems. He can be contacted at email: marwanesd448@gmail.com.



Dhari Yousif Mahmood     is a Prof at the Department of Electrical Engineering at the University of Technology, Baghdad, Iraq. He was awarded his M.Sc and Ph.D. in Electrical Power Engineering from Sant.Peterburg Polytechnical Institute-Russa in 1986 and 1990 respectively. His BSc degree was received in 1981 from the University of Baghdad-Collage of Engineering-Iraq. He works in the field of renewable energy and power system analysis. He supervises a large number of postgraduate students in both masters and Ph.D. degrees. He can be contacted at email: dhari.y.mahmood@uotechnology.edu.iq.



Ali Hussein Numan     received the BSc, M.Sc, and Ph.D. in Electrical Engineering from the University of Technology, in 1999, 2003, and 2009, respectively. Currently, he is an Associate Professor of Electrical Engineering in the Electromechanical Engineering Department of the University of Technology (UoT). He has co-authored the textbook *Small and Special Electric Motor and Their Control Technique*, 2016, and published 37 journals and conferences papers. His research interests include power electronics, variable speed drives, renewable energy, and modeling and simulation. He can be contacted at email: ali.h.numan@uotechnology.edu.iq.